CMB Angular Power Spectra and their Likelihoods: in Theory and in (Planck) Practice

E. Hivon & S. Galli

Planck likelihood: A hybrid approach

- Low-ℓ (ℓ < 30):
  - **TT**: Pixel-based approach based on N_{side}=16 Commander component separated map, 92% sky, all Planck frequencies used+WMAP+Haslam
  - **TE and EE**: Pixel based approach based on Planck LFI 70GHz map, 46% of the sky. 30 GHz and 353GHz used for foreground cleaning.

- High-ℓ (30 < ℓ < 2500):
  - **TT**: Gaussian likelihood based on HFI 100, 143, 217GHz at (70, 60, 50% sky)
  - **TE,EE**: Gaussian likelihood, HFI 100, 143, 217GHz at (70, 50, 40% sky).

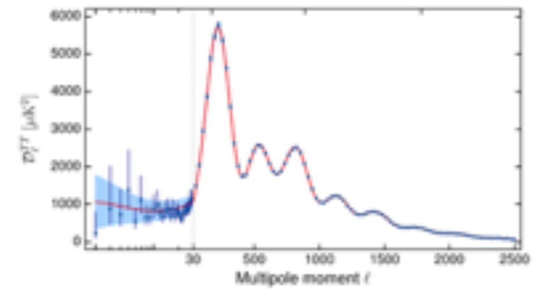

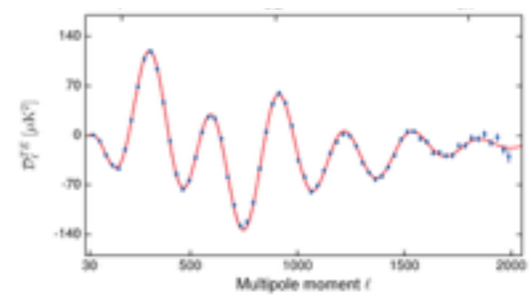

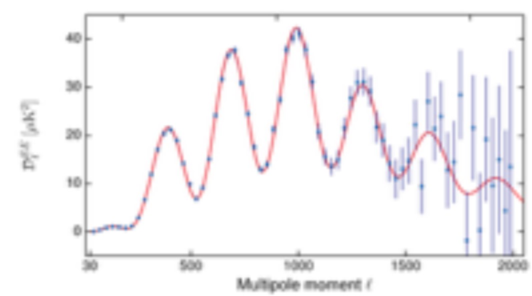

Planck 2015 results. XI.

Planck 2015 results

XI. CMB power spectra, likelihoods, and robustness of parameters

Planck Collaboration: N. Aghanim[63], M. Arnaud[78], M. Ashdown[74,6], J. Aumont[63], C. Baccigalupi[91], A. J. Banday[103,10], R. B. Barreiro[69], J. G. Bartlett[1,71], N. Bartolo[32,70], E. Battaner[105,106], K. Benabed[64,102], A. Benoît[61], A. Benoit-Lévy[24,64,102], J.-P. Bernard[103,10], M. Bersanelli[35,51], P. Bielewicz[86,10,91], J. J. Bock[71,12], A. Bonaldi[72], L. Bonavera[20], J. R. Bond[9], J. Borrill[15,96], F. R. Bouchet[64,94,*], F. Boulanger[63], M. Bucher[1], C. Burigana[50,33,52], R. C. Butler[50], E. Calabrese[98], J.-F. Cardoso[79,1,64], A. Catalano[80,77], A. Challinor[66,74,13], H. C. Chiang[28,7], P. R. Christensen[87,38], D. L. Clements[59], L. P. L. Colombo[23,71], C. Combet[80], A. Coulais[77], B. P. Crill[71,12], A. Curto[69,6,74], F. Cuttaia[50], L. Danese[91], R. D. Davies[72], R. J. Davis[72], P. de Bernardis[34], A. de Rosa[50], G. de Zotti[47,91], J. Delabrouille[1], F.-X. Désert[57], E. Di Valentino[64,94], C. Dickinson[72], J. M. Diego[69], K. Dolag[104,84], H. Dole[63,62], S. Donzelli[51], O. Doré[71,12], M. Douspis[63], A. Ducout[64,59], J. Dunkley[98], X. Dupac[40], G. Efstathiou[66], F. Elsner[24,64,102], T. A. Enßlin[84], H. K. Eriksen[67], J. Fergusson[13], F. Finelli[50,52], O. Forni[103,10], M. Frailis[49], A. A. Fraisse[28], E. Franceschi[50], A. Frejsel[87], S. Galeotta[49], S. Galli[73], K. Ganga[1], C. Gauthier[1,83], M. Gerbino[100,89,34], M. Giard[103,10], E. Gjerløw[67], J. González-Nuevo[20,69], K. M. Górski[71,107], S. Gratton[74,66], A. Gregorio[36,49,56], A. Gruppuso[50,52], J. E. Gudmundsson[100,89,28], J. Hamann[101,99], F. K. Hansen[67], D. L. Harrison[66,74], G. Helou[12], S. Henrot-Versillé[76], C. Hernández-Monteagudo[14,84], D. Herranz[69], S. R. Hildebrandt[71,12], E. Hivon[64,102], W. A. Holmes[71], A. Hornstrup[17], K. M. Huffenberger[26], G. Hurier[63], A. H. Jaffe[59], W. C. Jones[28], M. Juvela[27], E. Keihänen[27], R. Keskitalo[15], K. Kiiveri[27,45], J. Knoche[84], L. Knox[29], M. Kunz[18,63,3], H. Kurki-Suonio[27,45], G. Lagache[5,63], A. Lähteenmäki[2,45], J.-M. Lamarre[77], A. Lasenby[6,74], M. Lattanzi[33,53], C. R. Lawrence[71], M. Le Jeune[1], R. Leonardi[8], J. Lesgourgues[65,101], F. Levrier[77], A. Lewis[25], M. Liguori[32,70], P. B. Lilje[67], M. Lilley[64,94], M. Linden-Vørnle[17], V. Lindholm[27,45], M. López-Caniego[40], J. F. Macías-Pérez[80], B. Maffei[72], G. Maggio[49], D. Maino[35,51], N. Mandolesi[50,33], A. Mangilli[63,76], M. Maris[49], P. G. Martin[9], E. Martínez-González[69], S. Masi[34], S. Matarrese[32,70,42], P. R. Meinhold[30], A. Melchiorri[34,54], M. Migliaccio[66,74], M. Millea[29], S. Mitra[58,71], M.-A. Miville-Deschênes[63,9], A. Moneti[64], L. Montier[103,10], G. Morgante[50], D. Mortlock[59], S. Mottet[64,94], D. Munshi[93], J. A. Murphy[85], A. Narimani[22], P. Naselsky[88,39], F. Nati[28], P. Natoli[33,4,53], F. Noviello[72], D. Novikov[82], I. Novikov[87,82], C. A. Oxborrow[17], F. Paci[91], L. Pagano[34,54], F. Pajot[63], D. Paoletti[50,52], B. Partridge[44], F. Pasian[49], G. Patanchon[1], T. J. Pearson[12,60], O. Perdereau[76], L. Perotto[80], V. Pettorino[43], F. Piacentini[34], M. Piat[1], E. Pierpaoli[23], D. Pietrobon[71], S. Plaszczynski[76], E. Pointecouteau[103,10], G. Polenta[4,48], N. Ponthieu[63,57], G. W. Pratt[78], S. Prunet[64,102], J.-L. Puget[63], J. P. Rachen[21,84], M. Reinecke[84], M. Remazeilles[72,63,1], C. Renault[80], A. Renzi[37,55], I. Ristorcelli[103,10], G. Rocha[71,12], M. Rossetti[35,51], G. Roudier[1,77,71], B. Rouillé d'Orfeuil[76], J. A. Rubiño-Martín[68,19], B. Rusholme[60], L. Salvati[34], M. Sandri[50], D. Santos[80], M. Savelainen[27,45], G. Savini[90], D. Scott[22], P. Serra[63], L. D. Spencer[93], M. Spinelli[76], V. Stolyarov[6,97,75], R. Stompor[1], R. Sunyaev[84,95], D. Sutton[66,74], A.-S. Suur-Uski[27,45], J.-F. Sygnet[64], J. A. Tauber[41], L. Terenzi[92,50], L. Toffolatti[20,69,50], M. Tomasi[35,51], M. Tristram[76], T. Trombetti[50,33], M. Tucci[18], J. Tuovinen[11], G. Umana[46], L. Valenziano[50], J. Valiviita[27,45], F. Van Tent[81], P. Vielva[69], F. Villa[50], L. A. Wade[71], B. D. Wandelt[64,102,31], I. K. Wehus[71,67], D. Yvon[16], A. Zacchei[49], and A. Zonca[30]

(Affiliations can be found after the references)

Received 9 July 2015 / Accepted 18 May 2016

- Cl theory is simple, applying it to real data takes a lot of work
  Planck 2015 likelihood paper 99 pages, ~200 co-authors

Signal to noise

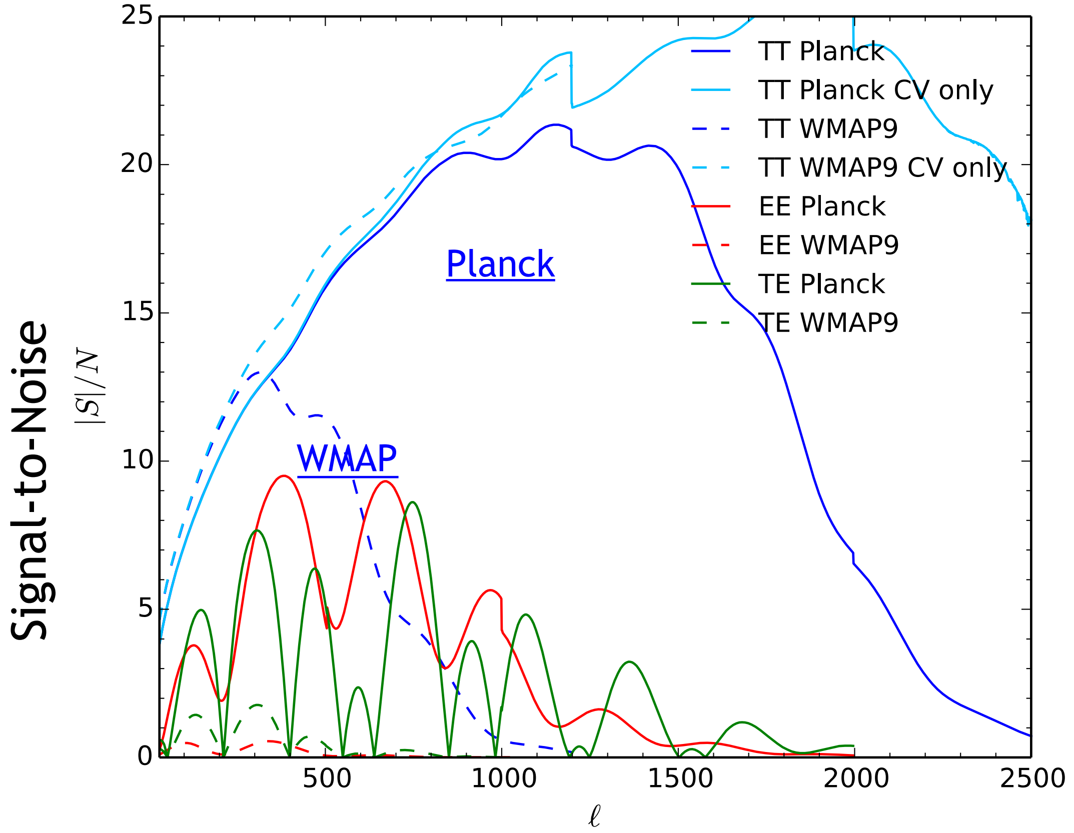

Planck sample variance limited till **l~1600** (data points till ~2500, fsky~40-70%)

WMAP sample variance limited till **l~600** (data points till l~1200)
ACT and SPT use < 5% of the sky.
Error bar due to sample variance ~3 times larger than Planck at l<1500!

From 2013 to 2015 data analysis

- Know your instrument
  - recalibration
  - 10x better beam knowledge
- Thou shalt commit (some) data alteration
  - remove "4K-cooler lines" from data
- Thou shalt covet more data
  - Polarisation !
  - Going from half-mission to full mission is good
  - Less correlated data splits are available

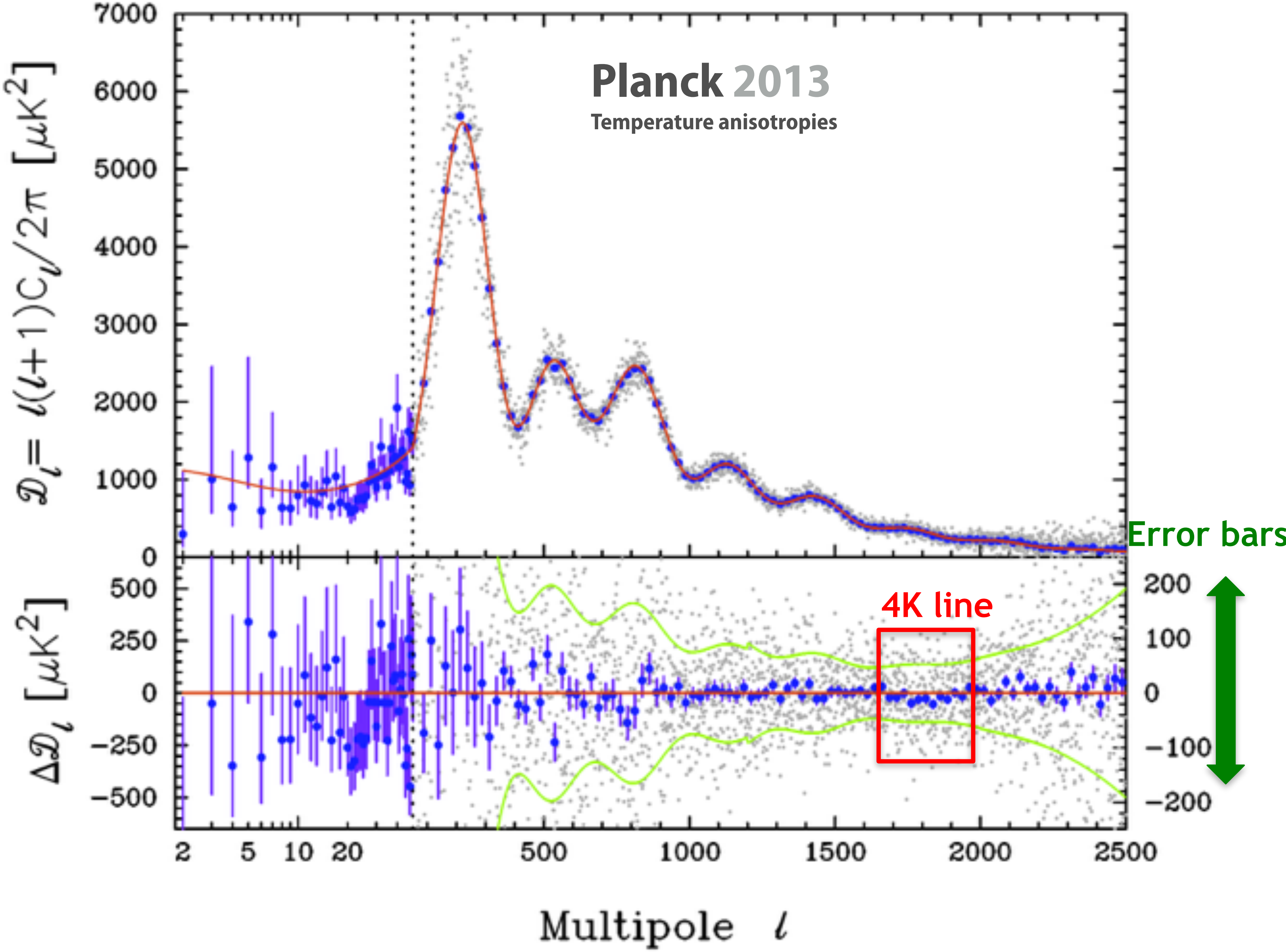

Planck 2013
Temperature anisotropies
$\mathcal{D}_\ell = \ell(\ell+1)C_\ell/2\pi \; [\mu K^2]$
$\Delta\mathcal{D}_\ell \; [\mu K^2]$
Multipole ℓ
Error bars
4K line

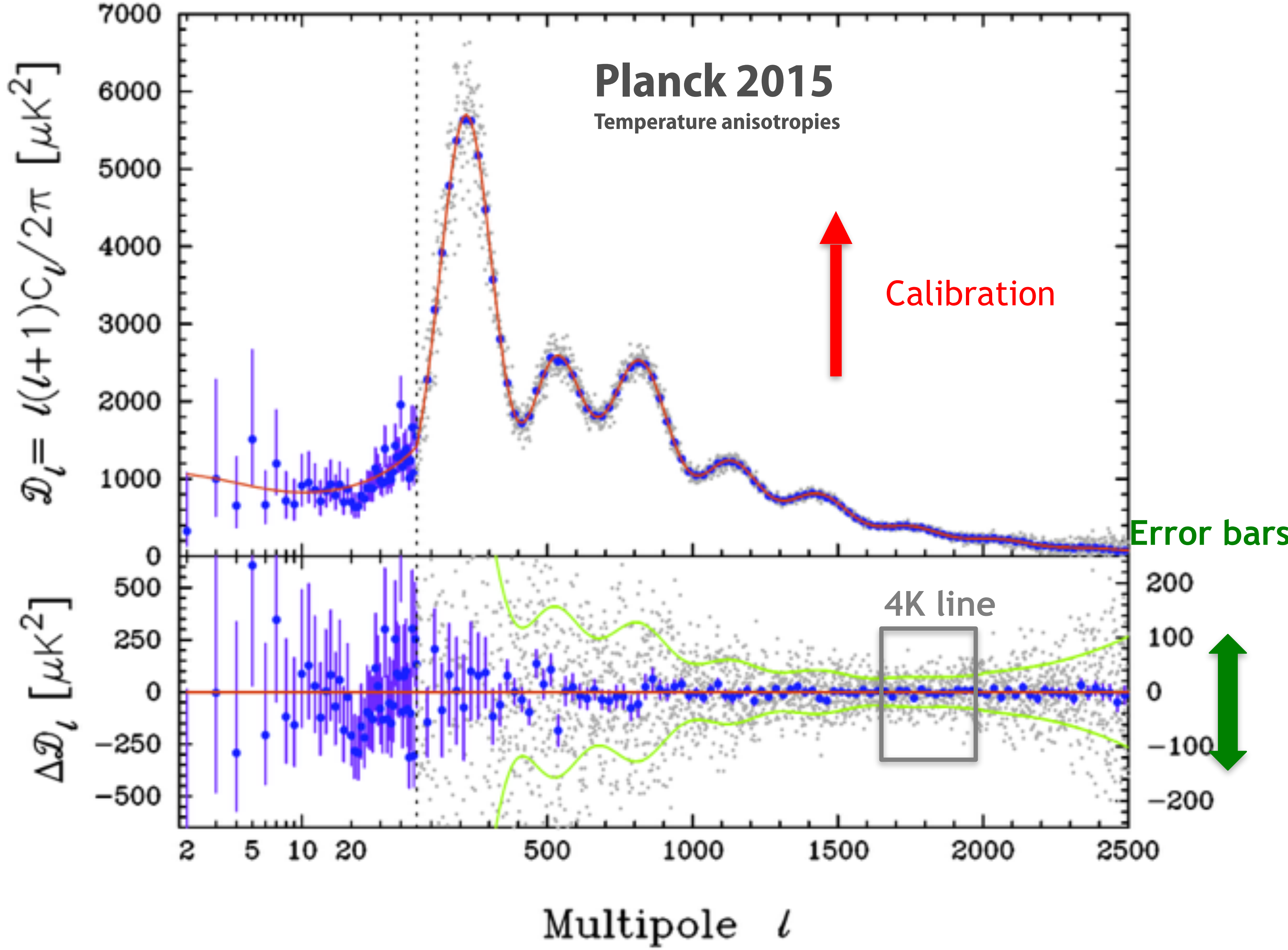

Planck 2015
Temperature anisotropies
Calibration
Error bars
4K line
$\mathcal{D}_\ell = \ell(\ell+1)C_\ell/2\pi\ [\mu K^2]$
$\Delta\mathcal{D}_\ell\ [\mu K^2]$
Multipole ℓ

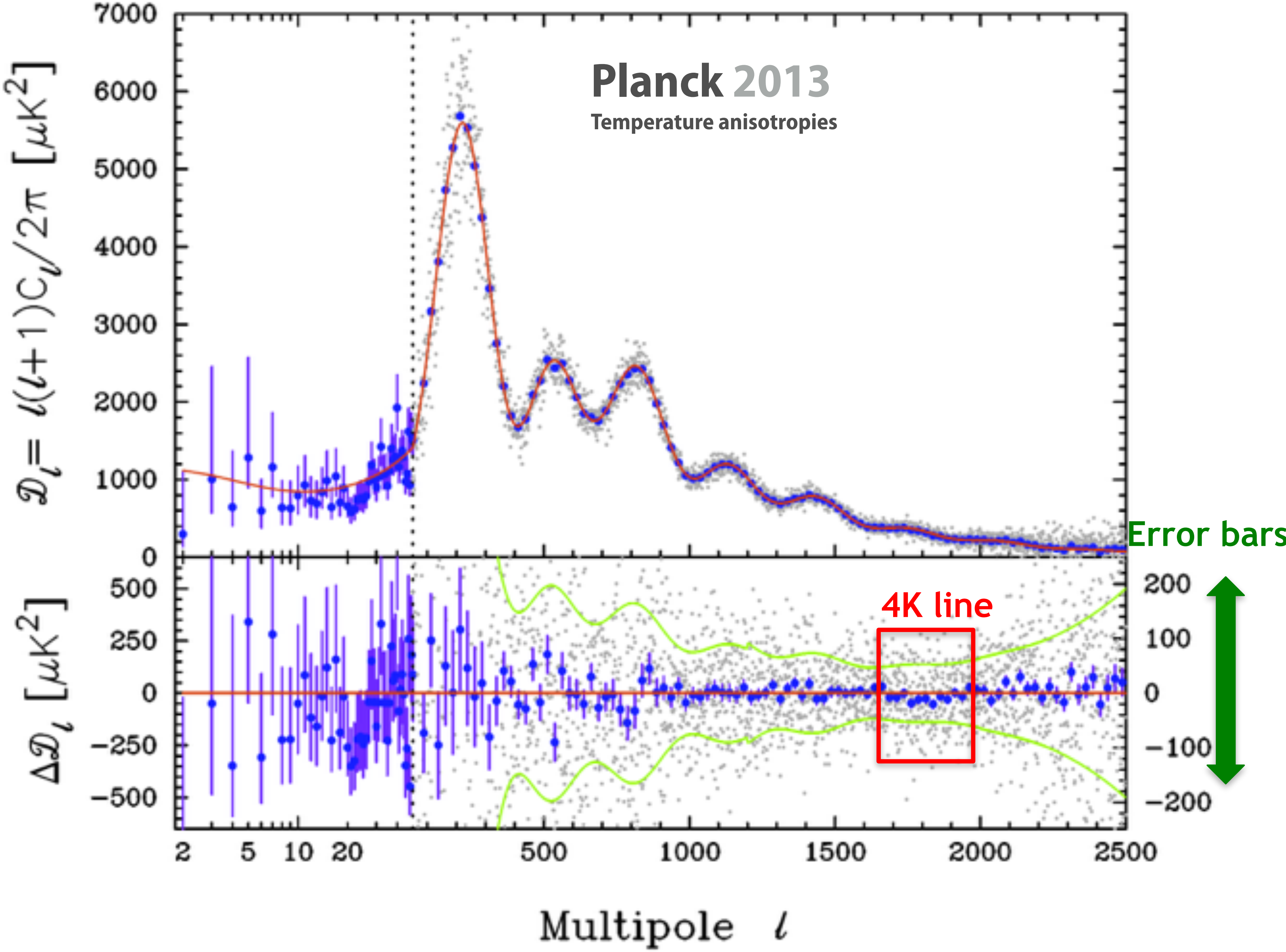

Planck 2013
Temperature anisotropies
$\mathcal{D}_\ell = \ell(\ell+1)C_\ell/2\pi\ [\mu K^2]$
$\Delta\mathcal{D}_\ell\ [\mu K^2]$
Multipole ℓ
Error bars
4K line

Datasets for the high-ℓ likelihood

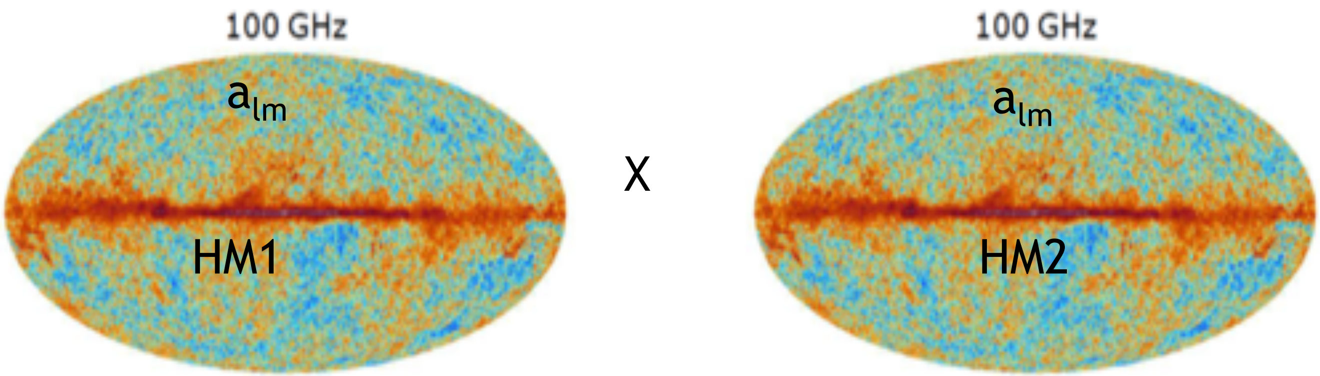

- 100, 143, 217GHz (best HFI channels for CMB).
  353 and 545 to estimate dust templates.
- Frequency maps from weighted average of all detectors at that frequency.
  Maps for each of the two temporal halves ~ 15 months of the total mission.
- Spectra only calculated correlating maps from two different half missions. Avoids noise bias, avoids correlating co-temporal systematics across detectors.

Planck 2015

- Data: $$\hat{C} = \left(\hat{C}^{TT}, \hat{C}^{EE}, \hat{C}^{TE}\right)$$

$$\hat{C}^{TT} = \left(\hat{C}^{TT}_{100\times100}, \hat{C}^{TT}_{143\times143}, \hat{C}^{TT}_{143\times217}, \hat{C}^{TT}_{217\times217}\right)$$

$$\hat{C}^{EE} = \left(\hat{C}^{EE}_{100\times100}, \hat{C}^{EE}_{100\times143}, \hat{C}^{EE}_{100\times217}, \hat{C}^{EE}_{143\times143}, \hat{C}^{EE}_{143\times217}, \hat{C}^{EE}_{217\times217}\right)$$

$$\hat{C}^{TE} = \left(\hat{C}^{TE}_{100\times100}, \hat{C}^{TE}_{100\times143}, \hat{C}^{TE}_{100\times217}, \hat{C}^{TE}_{143\times143}, \hat{C}^{TE}_{143\times217}, \hat{C}^{TE}_{217\times217}\right).$$

$$-\ln \mathcal{L}(\widehat{\mathbf{C}}|\mathbf{C}(\{\Omega\})) = \frac{1}{2}\left[\widehat{\mathbf{C}} - \mathbf{C}(\{\Omega\})\right]^T \mathbf{M}^{-1}\left[\widehat{\mathbf{C}} - \mathbf{C}(\{\Omega\})\right] + \text{const.}$$

Planck 2015

- Covariance matrix:

$$\mathbf{C} = \begin{pmatrix} C^{TTTT} & C^{TTEE} & C^{TTTE} \\ C^{EETT} & C^{EEEE} & C^{EETE} \\ C^{TETT} & C^{TEEE} & C^{TETE} \end{pmatrix}$$

$$C^{TTTT} = \left(\begin{array}{c|c|c|c} (100\times100)\times(100\times100) & (100\times100)\times(143\times143) & (100\times100)\times(217\times217) & (100\times100)\times(143\times217) \\ \hline (143\times143)\times(100\times100) & (143\times143)\times(143\times143) & (143\times143)\times(217\times217) & (143\times143)\times(143\times217) \\ \hline (217\times217)\times(100\times100) & (217\times217)\times(143\times143) & (217\times217)\times(217\times217) & (217\times217)\times(143\times217) \\ \hline (143\times217)\times(100\times100) & (143\times217)\times(143\times143) & (143\times217)\times(217\times217) & (143\times217)\times(143\times217) \end{array}\right).$$

Unbinned, this is a ~23000x23000 matrix!

Foreground model

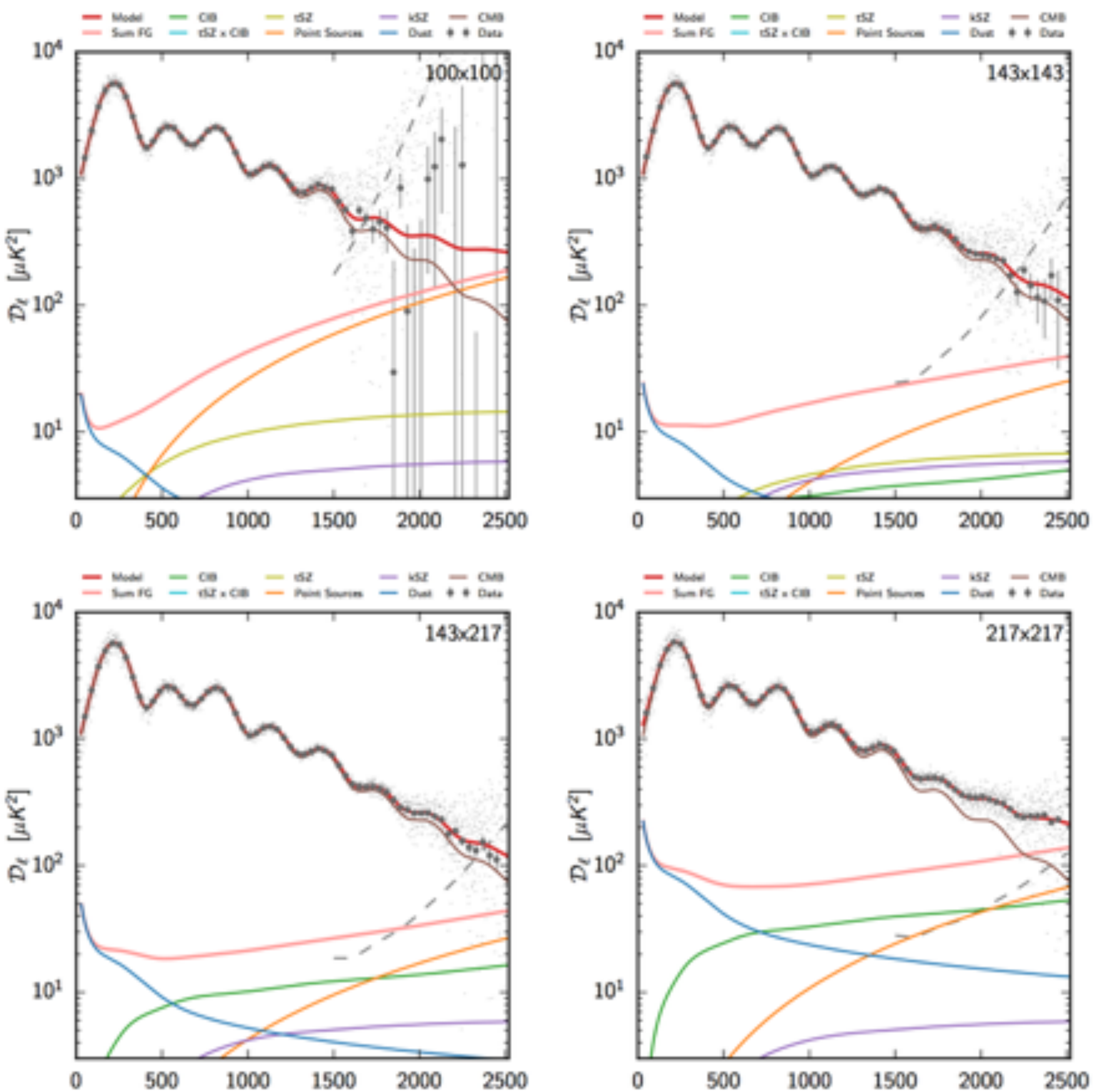

Planck 2015 results. XI.

- We mask regions of the sky most contaminated by dust, CO and extragalactic point sources. We retain 66, 57, 47% at 100, 143, 217GHz.
- We model the foregrounds in the remaining sky at the power spectrum level.
  - Galactic dust
  - Unresolved Point sources
  - Clustered CIB-cosmic infrared background
  - Thermal and Kinetic Sunyaev-Zeldovich from galaxy clusters
  - Cross-correlation between tSZxCIB

Foregrounds

- Dust
  - ✦ TT: use 545GHz C_ℓ modelled (via difference of masks) as dust + CIB + PS
    TE and EE: use 353GHz instead
  - ✦ Subtract $A_{\nu 1 \nu 2}\, C_\ell^{DUST}(n)$ template from all cross-spectra, with a free amplitude, and free spectral slope, which are marginalised over
- Unresolved Point sources
  - ✦ TT only: flat spectrum fit on $C\ell$

Table 10. Parameters used for astrophysical foregrounds and instrumental modelling.

Parameter	Prior range	Definition
A^{PS}_{100}	[0, 400]	Contribution of Poisson point-source power to $\mathcal{D}^{100\times100}_{3000}$ for *Planck* (in μK^2)
A^{PS}_{143}	[0, 400]	As for A^{PS}_{100} but at 143 GHz
A^{PS}_{217}	[0, 400]	As for A^{PS}_{100} but at 217 GHz
$A^{PS}_{143\times217}$	[0, 400]	As for A^{PS}_{100} but at 143 × 217 GHz
A^{CIB}_{217}	[0, 200]	Contribution of CIB power to $\mathcal{D}^{217}_{3000}$ at the *Planck* CMB frequency for 217 GHz (in μK^2)
A^{tSZ}	[0, 10]	Contribution of tSZ to $\mathcal{D}^{143\times143}_{3000}$ at 143 GHz (in μK^2)
A^{kSZ}	[0, 10]	Contribution of kSZ to $\mathcal{D}_{3000}$ (in μK^2)
$\xi^{tSZ\times CIB}$	[0, 1]	Correlation coefficient between the CIB and tSZ
A^{dustTT}_{100}	[0, 50] (7 ± 2)	Amplitude of Galactic dust power at $\ell = 200$ at 100 GHz (in μK^2)
A^{dustTT}_{143}	[0, 50] (9 ± 2)	As for A^{dustTT}_{100} but at 143 GHz
$A^{dustTT}_{143\times217}$	[0, 100] (21 ± 8.5)	As for A^{dustTT}_{100} but at 143 × 217 GHz
A^{dustTT}_{217}	[0, 400] (80 ± 20)	As for A^{dustTT}_{100} but at 217 GHz
c_{100}	[0, 3] (0.9990004 ± 0.001)	Power spectrum calibration for the 100 GHz
c_{217}	[0, 3] (0.99501 ± 0.002)	Power spectrum calibration for the 217 GHz
y_{cal}	[0.9, 1.1] (1 ± 0.0025)	Absolute map calibration for *Planck*
A^{dustEE}_{100}	[0, 10] (0.06 ± 0.012)	Amplitude of Galactic dust power at $\ell = 500$ at 100 GHz (in μK^2)
$A^{dustEE}_{100\times143}$	[0, 10] (0.05 ± 0.015)	As for A^{dustEE}_{100} but at 100 × 143 GHz
$A^{dustEE}_{100\times217}$	[0, 10] (0.11 ± 0.033)	As for A^{dustEE}_{100} but at 100 × 217 GHz
A^{dustEE}_{143}	[0, 10] (0.1 ± 0.02)	As for A^{dustEE}_{100} but at 143 GHz
$A^{dustEE}_{143\times217}$	[0, 10] (0.24 ± 0.048)	As for A^{dustEE}_{100} but at 143 × 217 GHz
A^{dustEE}_{217}	[0, 10] (0.72 ± 0.14)	As for A^{dustEE}_{100} but at 217 GHz
A^{dustTE}_{100}	[0, 10] (0.14 ± 0.042)	Amplitude of Galactic dust power at $\ell = 500$ at 100 GHz (in μK^2)
$A^{dustTE}_{100\times143}$	[0, 10] (0.12 ± 0.036)	As for A^{dustTE}_{100} but at 100 × 143 GHz
$A^{dustTE}_{100\times217}$	[0, 10] (0.3 ± 0.09)	As for A^{dustTE}_{100} but at 100 × 217 GHz
A^{dustTE}_{143}	[0, 10] (0.24 ± 0.072)	As for A^{dustTE}_{100} but at 143 GHz
$A^{dustTE}_{143\times217}$	[0, 10] (0.6 ± 0.18)	As for A^{dustTE}_{100} but at 143 × 217 GHz
A^{dustTE}_{217}	[0, 10] (1.8 ± 0.54)	As for A^{dustTE}_{100} but at 217 GHz

Notes. The columns indicate the symbol for each parameter, the prior used for exploration (square brackets denote uniform priors, parentheses indicate Gaussian priors), and definitions. Beam eigenmode amplitudes require a correlation matrix to fully describe their joint prior and so do not appear in the table; they are internally marginalized over rather than explicitly sampled. This table only lists the instrumental parameters that are explored in the released version, but we do consider more parameters to assess the effects of beam uncertainties and beam leakage; see Sect. 3.4.3.

Many non-cosmological parameters

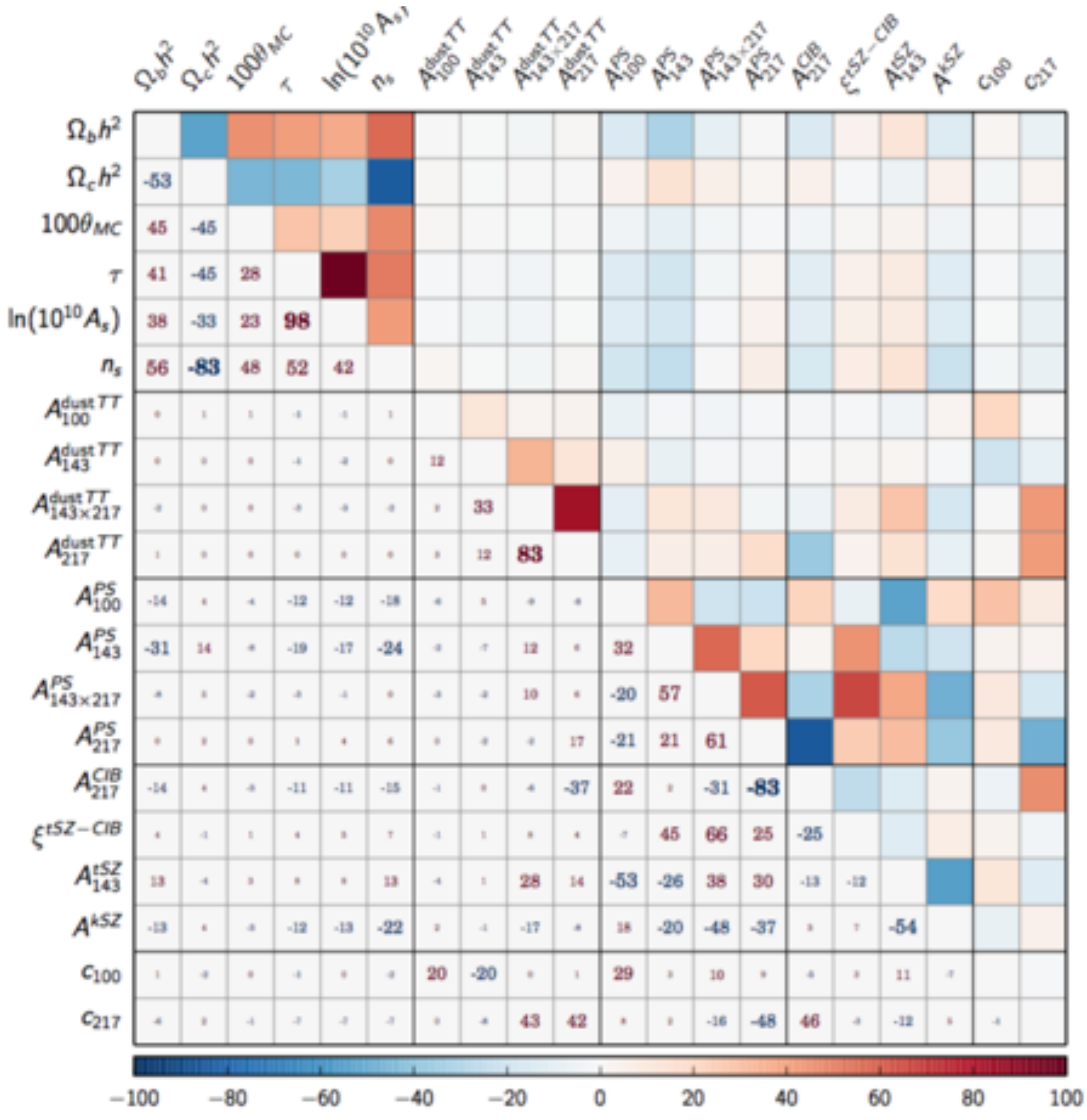

Correlated noise seen in detector sets (simultaneous observations) used in 2013 analysis

Half-ring maps of detsets: $(HR1\text{-}HR2)_{DS1}$ X $(HR1\text{-}HR2)_{DS2}$ provide a correlated noise template added to cosmological analysis

No correlation seen in Half-Mission used in 2015, but deviation from white noise included in S+N covariance matrix calculation

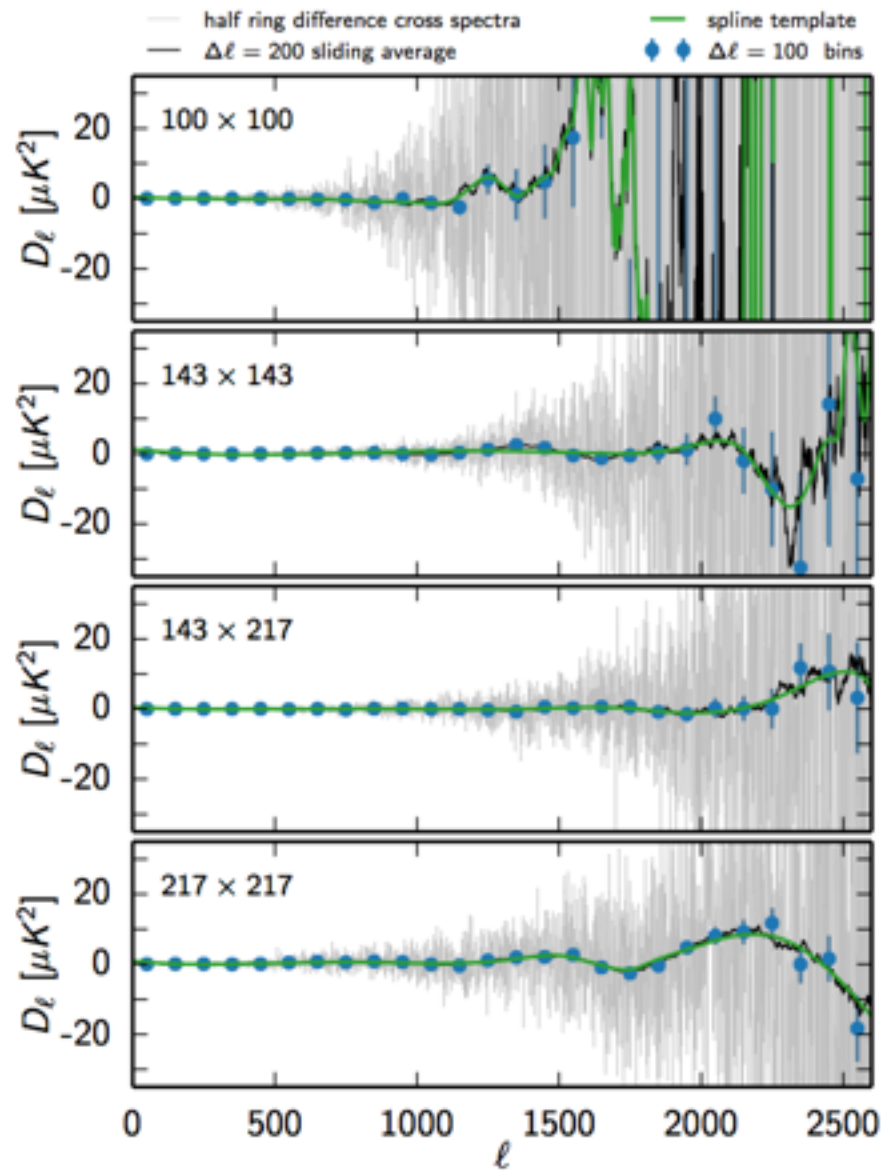

Systematics

- Comparison of some systematics with statistical errors

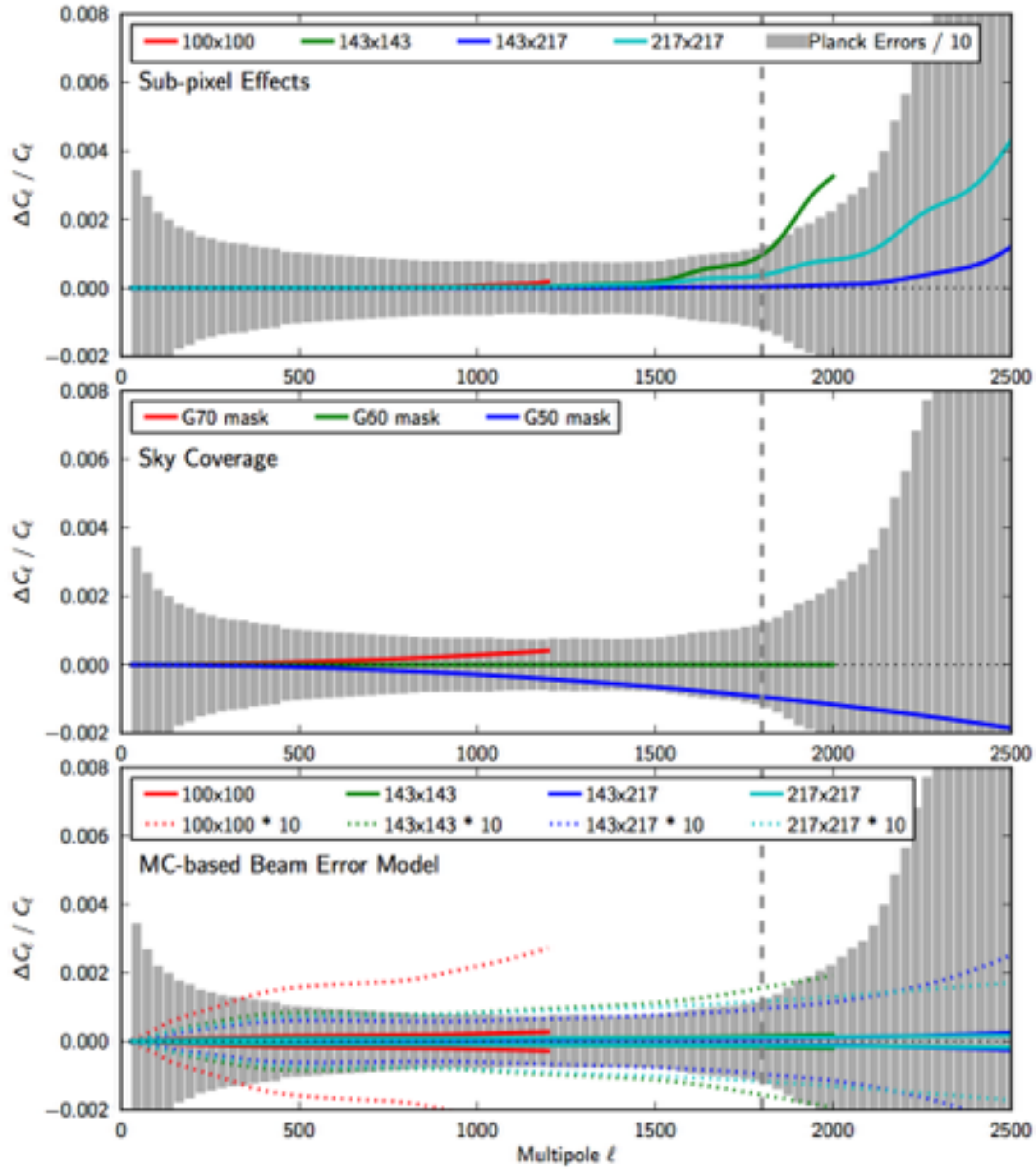

Inter-frequency differences

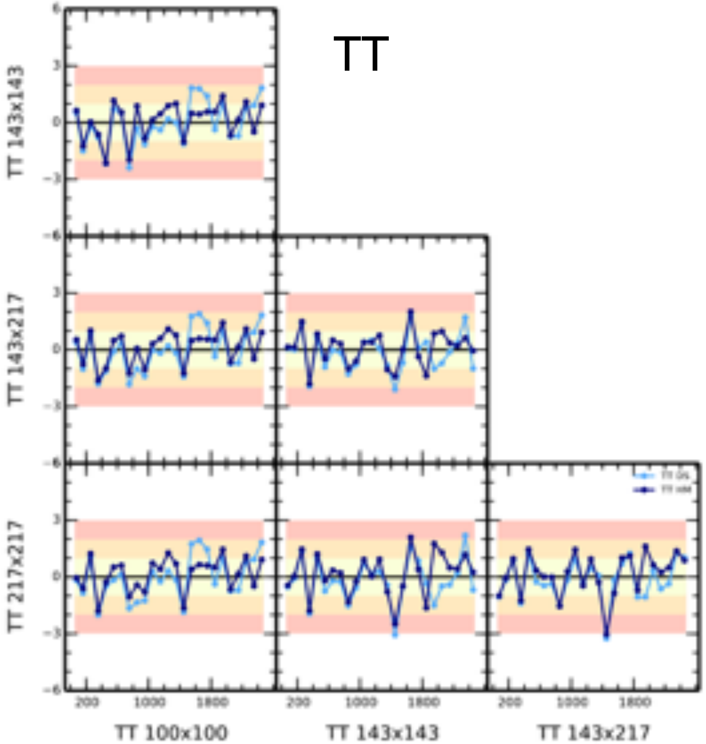

TT behaves very well

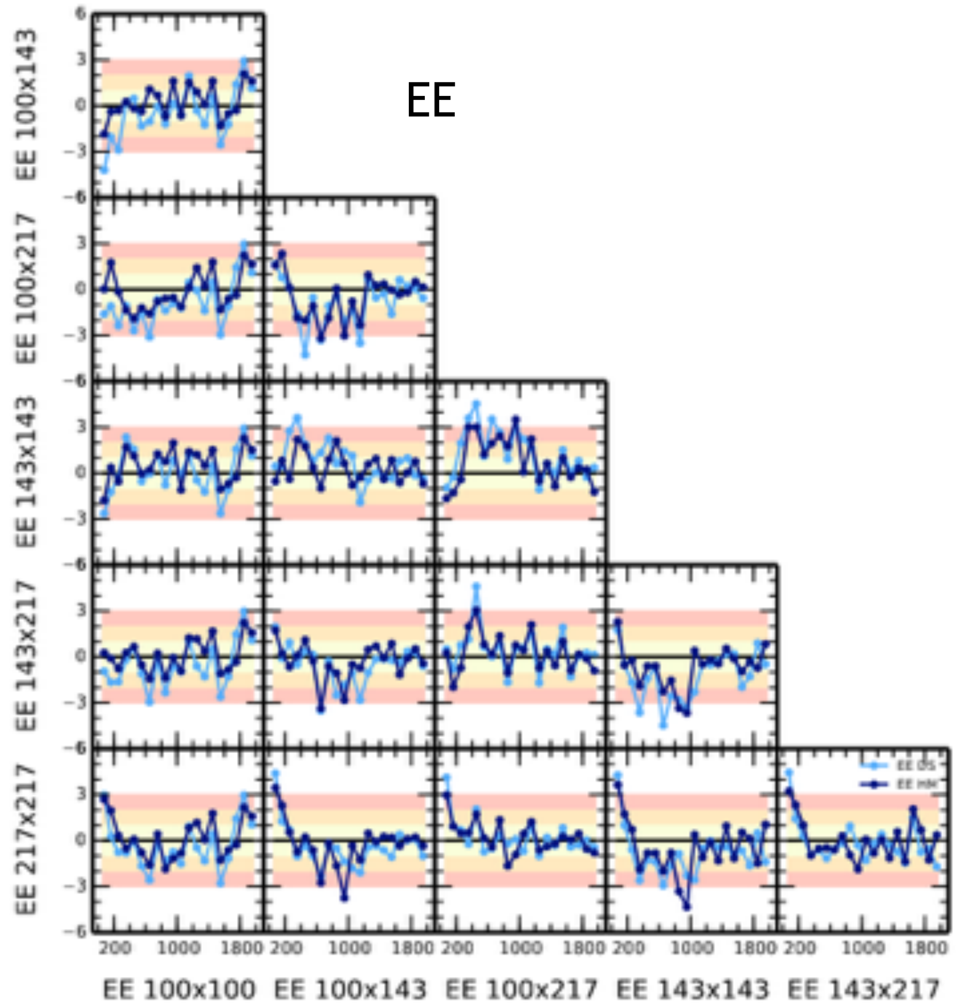

Frequency redundancy allows us to check foregrounds cleaning and systematics.

TE and EE too large deviations. A sign of remaining systematics.

Planck 2015 results. XI.

Inter-frequency differences

TT

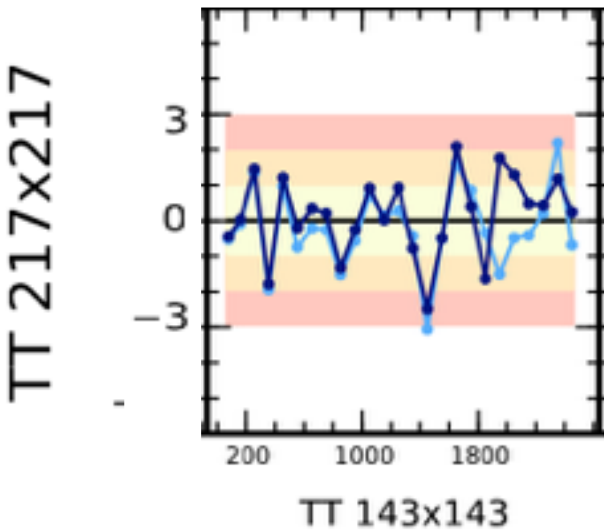

TT behaves very well

EE

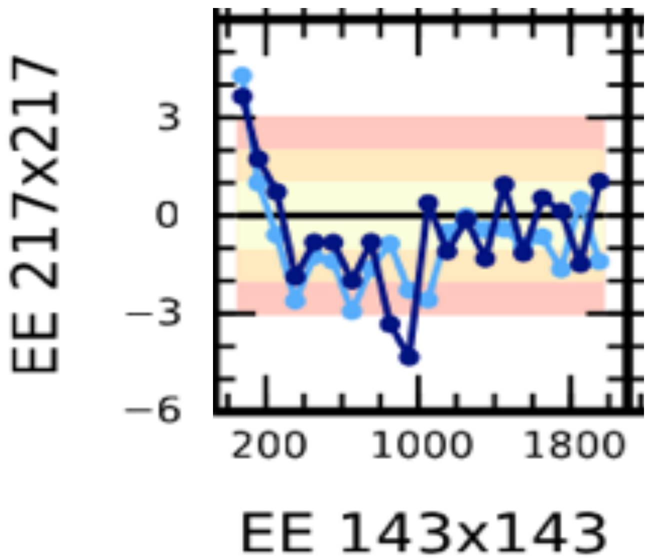

TE and EE too large deviations. A sign of remaining systematics.

Frequency redundancy allows us to check foregrounds cleaning and systematics.

Planck 2015 results. XI.

Beam related systematics

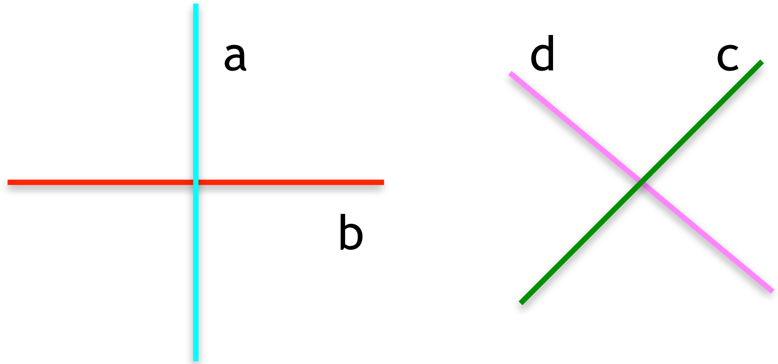

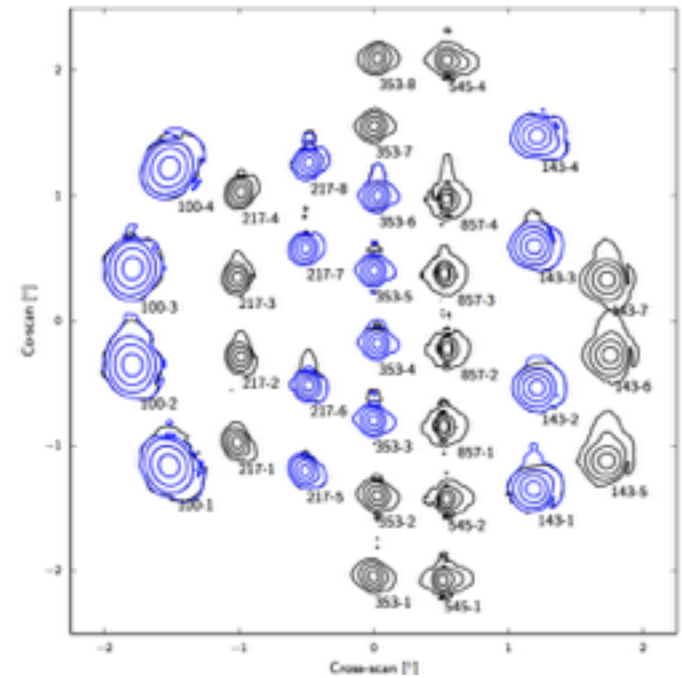

$$I = \langle E_x^2 \rangle + \langle E_y^2 \rangle = \langle E_{45}^2 \rangle + \langle E_{-45}^2 \rangle$$

$$Q = \langle E_x^2 \rangle - \langle E_y^2 \rangle = I_a - I_b$$

$$U = 2\langle E_x E_y \rangle = \langle E_{45}^2 \rangle - \langle E_{-45}^2 \rangle = I_c - I_d$$

- In the absence of polarisation modulation (eg rotating half-wave plate, rHWP*), polarisation is obtained by differencing 2 different orthogonal detectors ➔ any detector mismatch (in gains, beams, band-passes, …) creates fake polarisation (Hu et al, 2003, and many others).

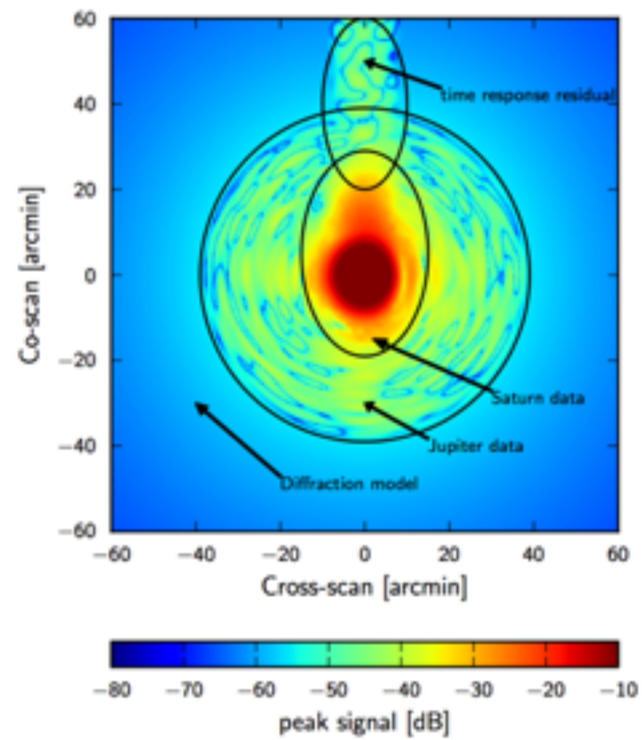

Note: *rHWP are still little used, and create their own kind of problems (Takakura et al, 2017)

QuickPol

- **Temperature QuickBeam** (used in 2013 and 2015 analyses):
  - ✦ $C'^{TT}_{\ell} = \Sigma_s \, \omega_s^2 \; b^*_{\ell s} \; b_{\ell s} \; C^{TT}_{\ell}$
    - $b_{\ell s}$: weighted combination of scanning beams in DetSet,
    - ω_s^2: encodes scanning strategy (assumed to vary slowly across the sky)

s=2

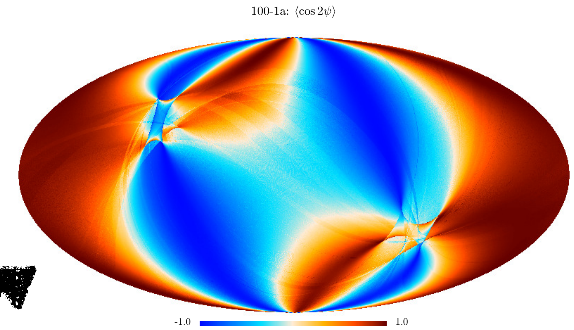

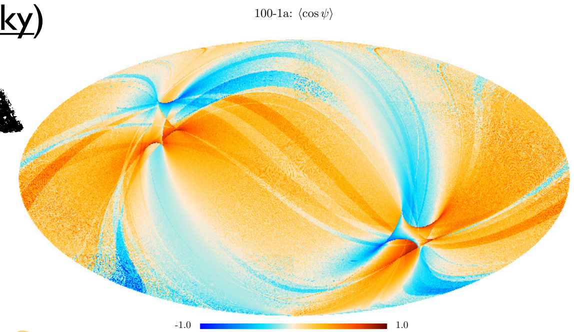

s=1

- **Temperature + Polarisation QuickPol** (in 2017 analysis):
  - ✦ $\mathbf{C'_{\ell}} = \Sigma_{sij} \; \mathbf{\Omega}_{sij} \circledast \mathbf{B}^{*t}_{\ell s i} \, . \, \mathbf{C}_{\ell} \, . \, \mathbf{B}_{\ell s j}$
    - **C** : 3x3 *C(l)* matrix
    - **B** : weighted scanning polarised beams in DetSet or Half missions
    - **Ω** : encodes scanning strategy weighted by map-making IQU inverse covariance matrix

  - ✦ provides effective beam window matrix $\mathbf{W}_{\ell}$ describing C_{ℓ} coupling, **without numerical simulations !**
  - ✦ has be extended to gain and polar efficiency uncertainty
  - ✦ Backward *C(l)* fitting can then still be used as a rain check to detect/catch remaining systematics

Map(s) Power Spectra

Sky Power Spectra

$$\begin{pmatrix} \tilde{C}^{TT}_{\ell} \\ \tilde{C}^{EE}_{\ell} \\ \tilde{C}^{BB}_{\ell} \\ \tilde{C}^{TE}_{\ell} \\ \tilde{C}^{TB}_{\ell} \\ \tilde{C}^{EB}_{\ell} \\ \tilde{C}^{ET}_{\ell} \\ \tilde{C}^{BT}_{\ell} \\ \tilde{C}^{BE}_{\ell} \end{pmatrix} = \mathbf{W}_{\ell} \cdot \begin{pmatrix} C^{TT}_{\ell} \\ C^{EE}_{\ell} \\ C^{BB}_{\ell} \\ C^{TE}_{\ell} \\ C^{TB}_{\ell} \\ C^{EB}_{\ell} \end{pmatrix}$$

For each ℓ, $\mathbf{W}_{\ell}$ is a 9x6 (diagonal dominated) matrix

EH, Mottet, Ponthieu, 2017

Inter-frequency consistency:
fg corrected C(l)
143x143 - 100x100

Preliminary!

Ignoring beam leakage (2015 analysis)
With beam leakage prediction+correction (2017-8 analysis)

Spectacular improvement for TE !

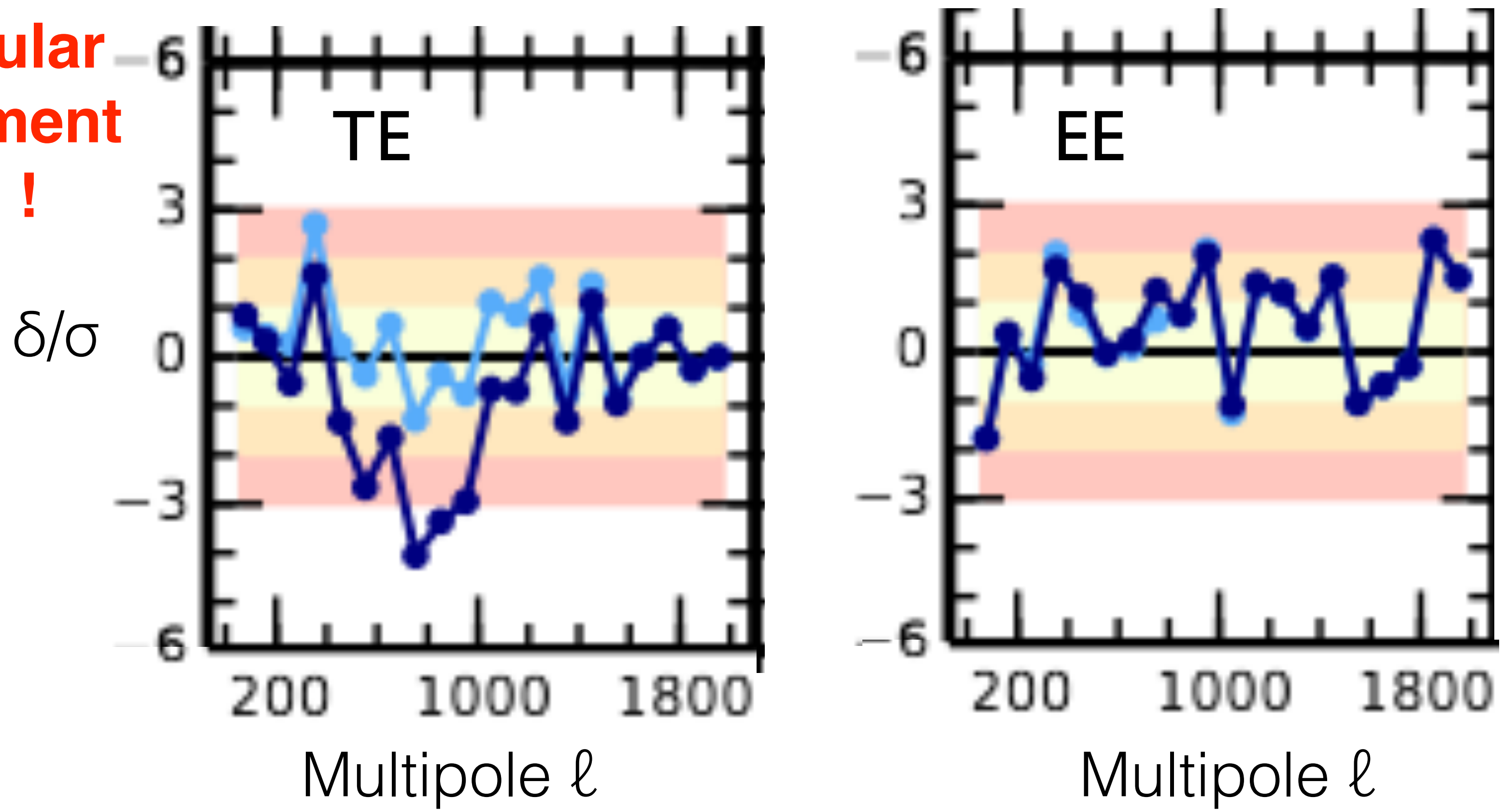

Covariance matrix

- Ingredients:
  - A fiducial CMB signal spectrum, based on your best estimate
  - Foreground fiducial models at relevant frequency, based on your best knowledge
  - A good estimate of the noise spectrum,
  - Systematics models and their uncertainty e.g. for Gaussian beam: $B_\ell = \exp(-\ell^2 (\sigma+\delta\sigma)^2)$
- Perform analytical calculations
- Validate with N_{sim} =10 000 Monte-Carlo simulations (see P. Natoli lecture)
  - limited accuracy $\Delta M_{ij} / M_{ii} M_{jj} \sim (2 / N_{sim})^{1/2} = 1\%$
  - mostly interesting for diagonal
- Apply to data,
- Repeat from step I

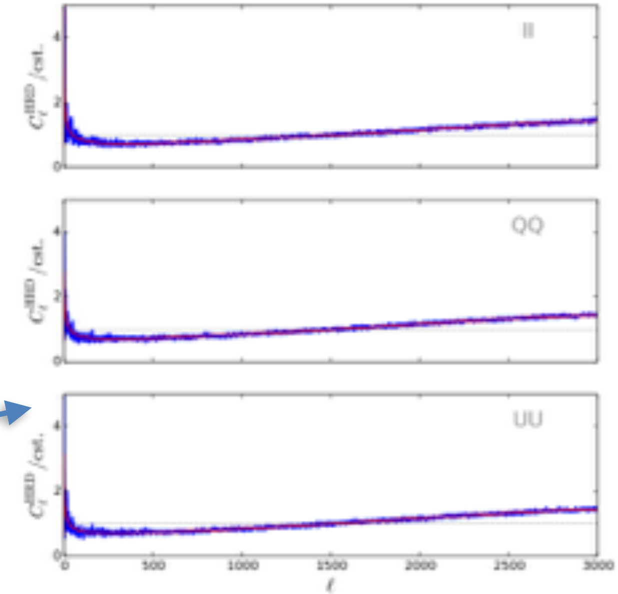

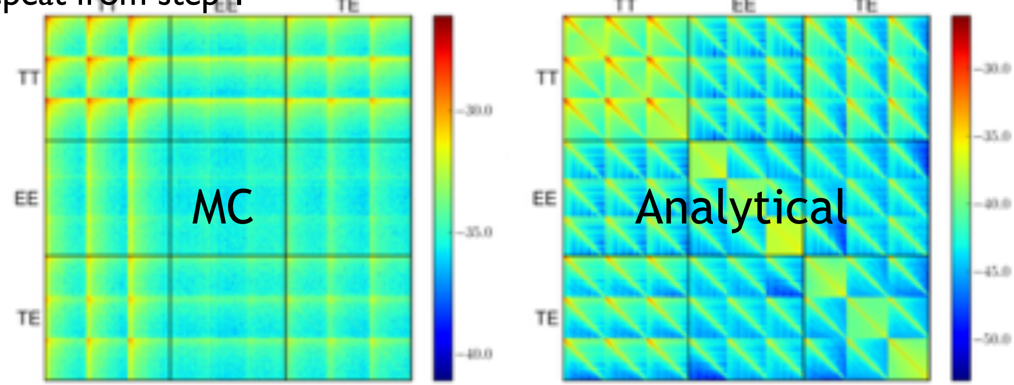

Point sources mask and C_ℓ

- In presence of a point source mask, the analytical computation of the covariance matrix (Efstathiou, 2004) that works fine for galactic masks, differ from Monte-Carlo based estimates, by up to 10 or 20%
- However, a new formalism, treating the point source 'holes' as a Poisson process, agrees much better with simulations (on going work with A. Challinor, F. Elsner, S.Gratton, M. Lilley & M. Migliaccio)

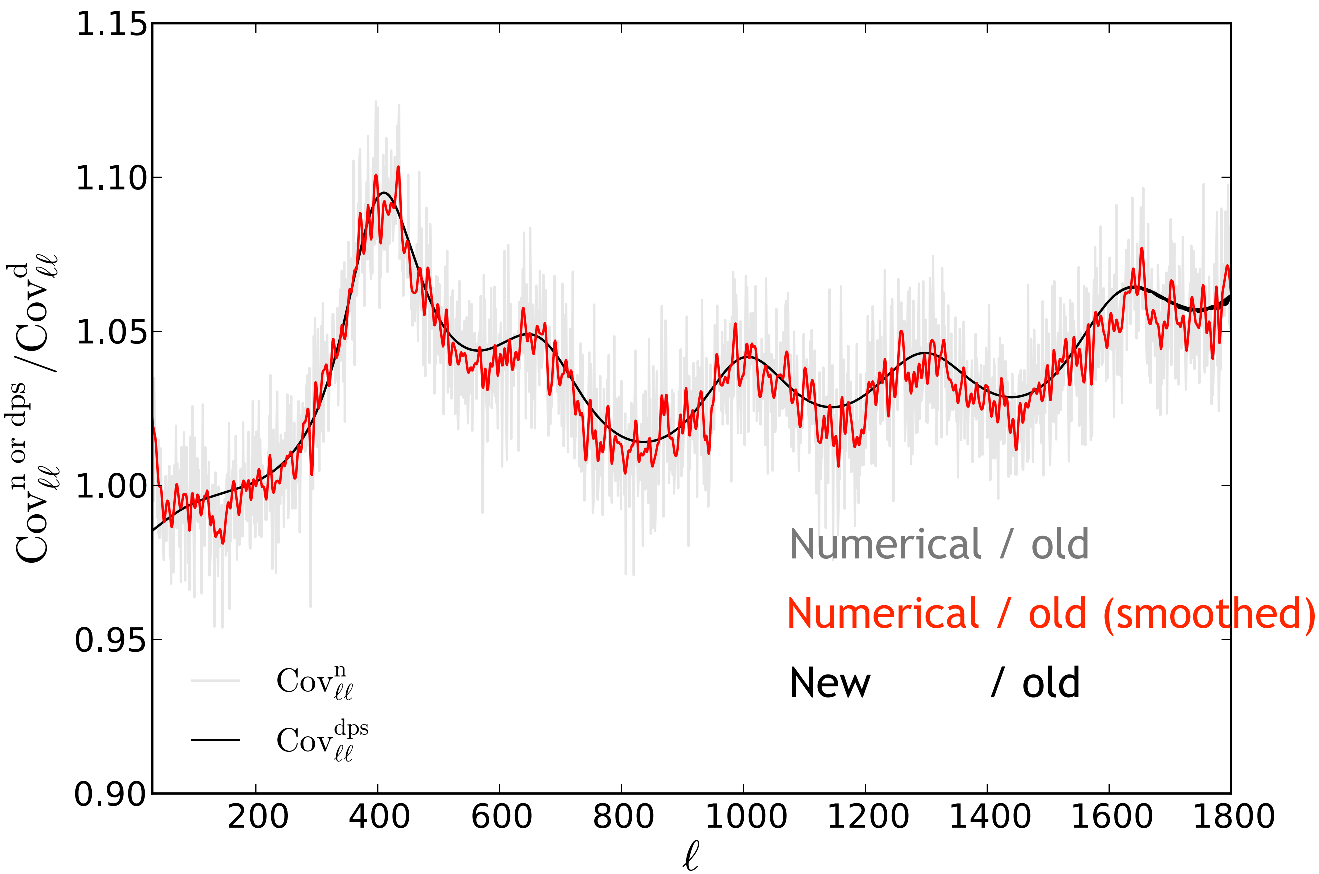

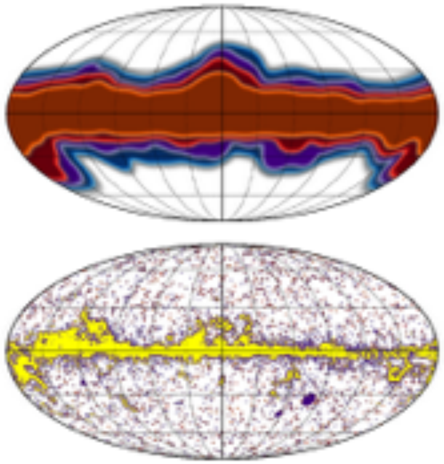

Validation

- tests, tests, and tests

Test impact of various settings on final parameters

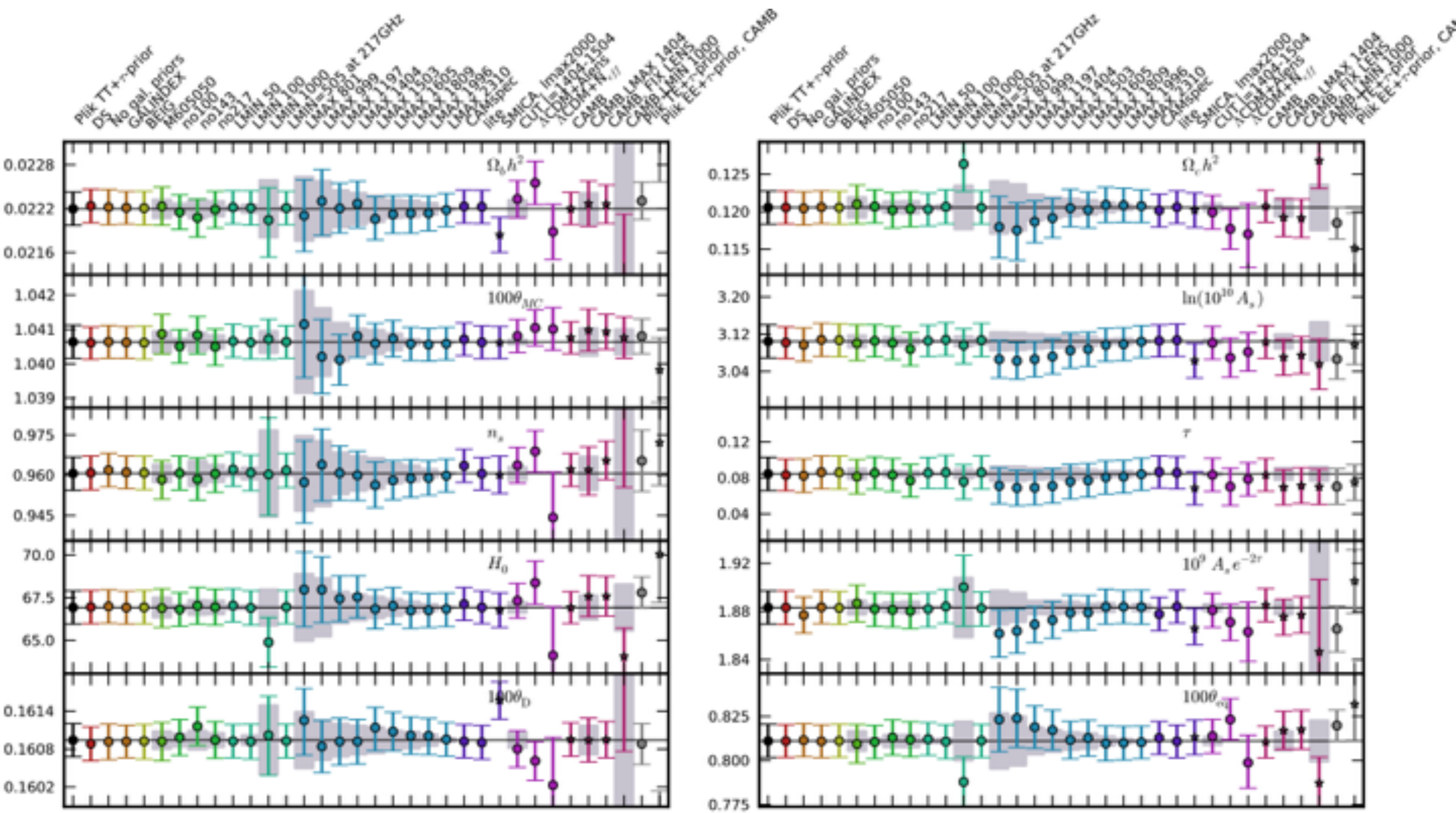

Planck 2015 results. XI.

Tests final parameters of 300 end-to-end simulations

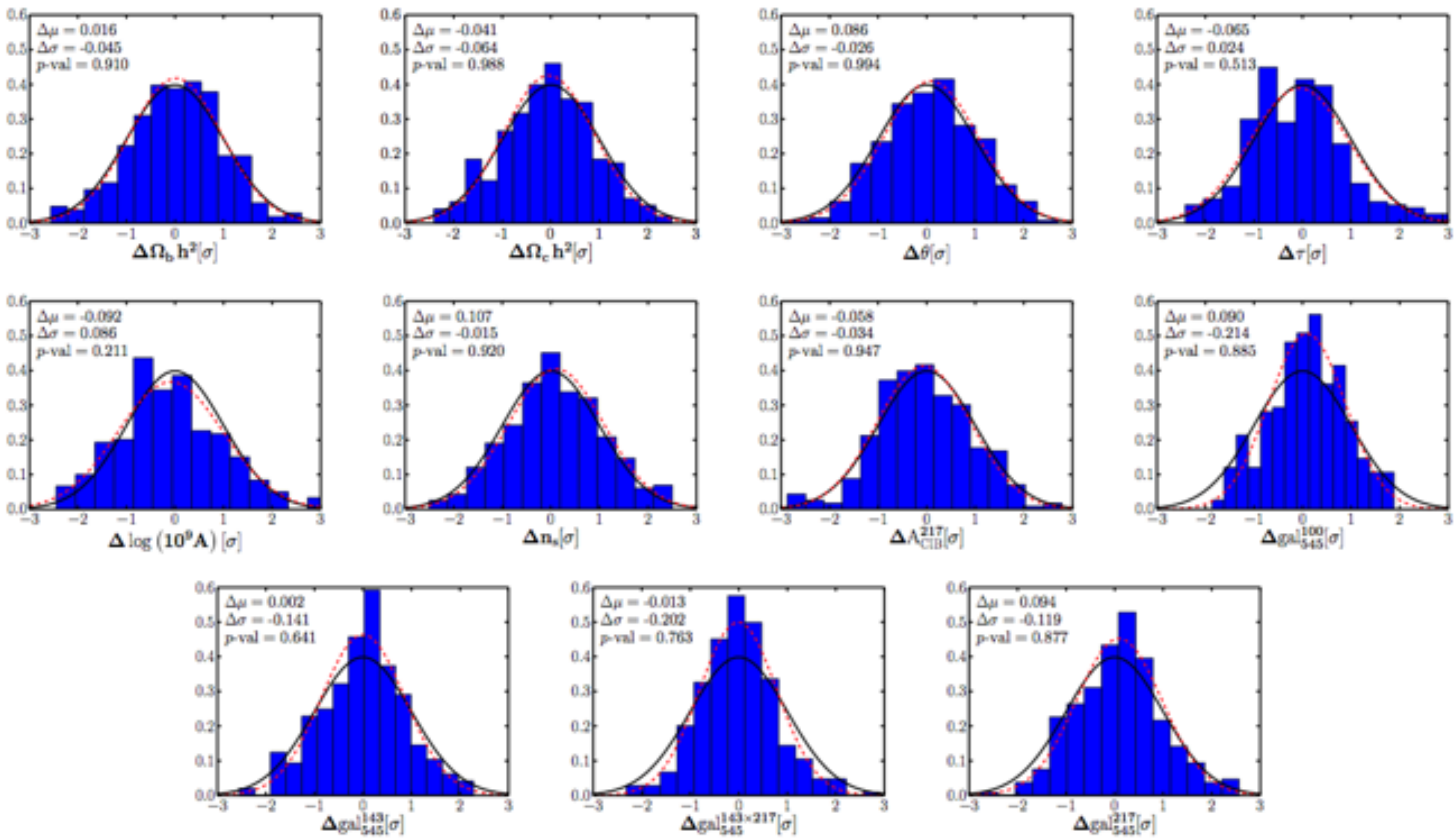

Final $C\ell$ and residuals

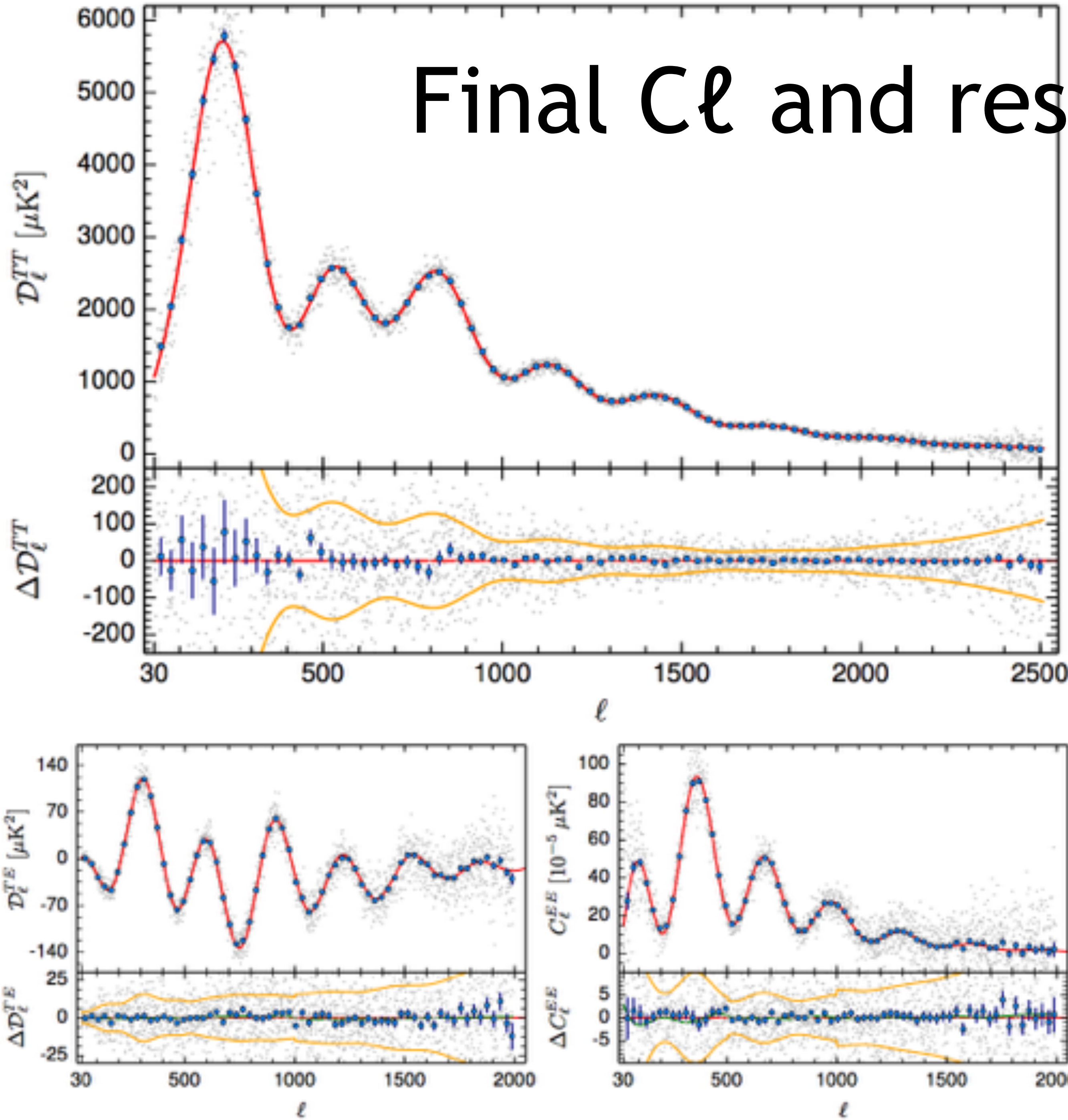

ΛCDM results from TT

[1] Parameter	2013N(DS)	2015F(CHM) (Plik)
$100\theta_{MC}$	1.04131 ± 0.00063	1.04086 ± 0.00048
$\Omega_b h^2$	0.02205 ± 0.00028	0.02222 ± 0.00023
$\Omega_c h^2$	0.1199 ± 0.0027	0.1199 ± 0.0022
H_0	67.3 ± 1.2	67.26 ± 0.98
n_s	0.9603 ± 0.0073	0.9652 ± 0.0062
Ω_m	0.315 ± 0.017	0.316 ± 0.014
σ_8	0.829 ± 0.012	0.830 ± 0.015
τ	0.089 ± 0.013	0.078 ± 0.019
$10^9 A_s e^{-2\tau}$	1.836 ± 0.013	1.881 ± 0.014

-1 sigma shift
30% weaker constraint

+3.5 sigma shift

2013=Planck Nominal 2013 TT+low-l WMAP polarization
2015=Planck Full 2015 TT+low-l Planck LFI polarization.

- Very good consistency between 2013-2015.
- Error bars improved by ~30%
- Calibration change shifts $10^9 A_s e^{-2\tau}$.
- 2015 constraint on optical depth weaker and lower than 2013. We use large scale polarization from Planck LFI !
- LCDM is an excellent fit to the data!

Planck 2015 results. XIII.

Planck 2015 Polarization at high-ℓ

Excellent agreement between TT, TE and EE

Despite remaining uncharacterized systematics in polarization at muK^2 level

Improvement in error bars up to 50%

Some parameters determined from TE as precisely as from TT.

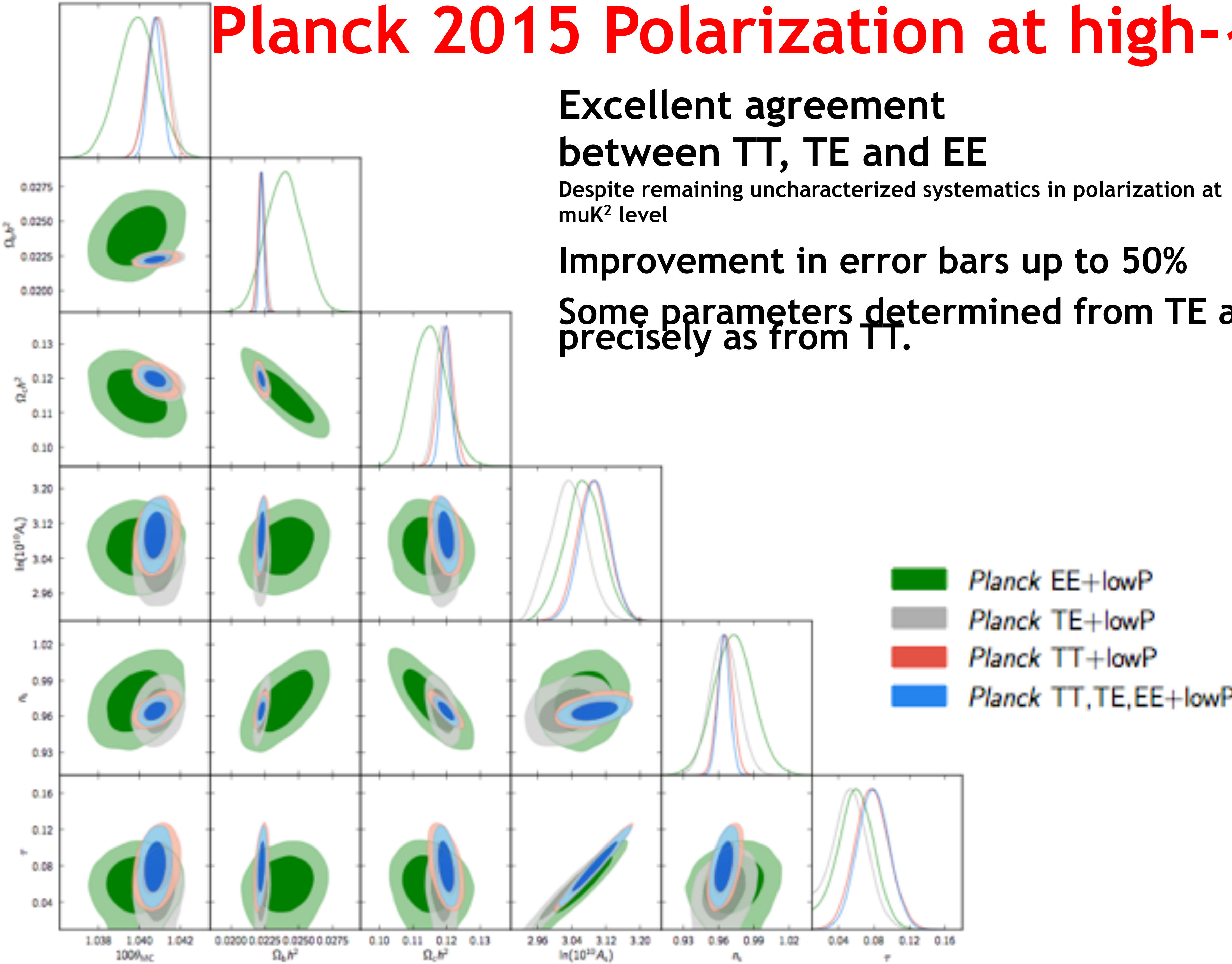

WMAP and Planck cosmologies

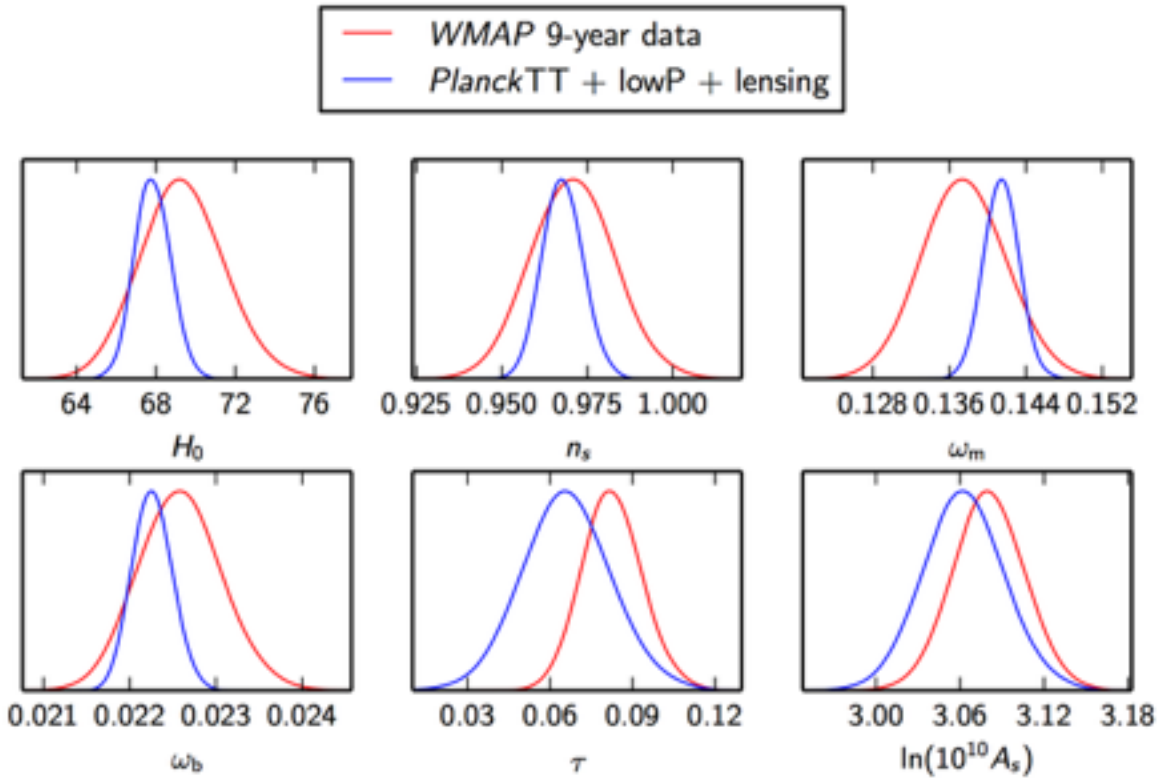

Hubble parameter [Km/s/Mpc]

Planck	67.8 ± 0.92
WMAP	69.7 ± 2.1

- WMAP and Planck parameters differ by ~1 $\text{sigma}_{\text{WMAP}}$.
- WMAP errors factor 2 larger than Planck.

Compare apples to apples

- Same prior on the optical depth, temperature only, same multipole region (although noise properties and fsky are still different).

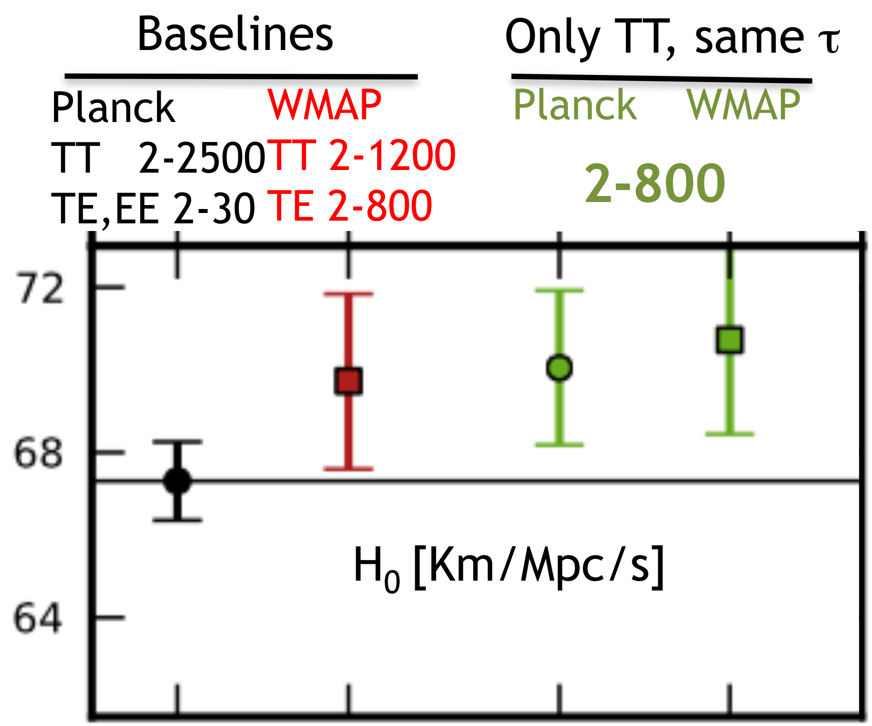

- Planck and WMAP agree very well when compared properly

- **Still need to prove that shifts between lmax=800 and lmax=2500 for Planck itself are consistent with expectations!**

Recipes for successful CMB analysis

- To deal with **foregrounds**:
  - ✦ mask the most affected pixels,
  - ✦ then make a parametric fit of the remaining foreground Cl (where the foreground is dominant) using frequency differences, or masks differences, or a priori models,
  - ✦ then marginalise over the fit parameters.
- Poor knowledge of the **instrument**:
  - ✦ add as many free parameters as necessary, and fit and/or marginalise them (eg, polar efficiency, relative calibration with respect to 143GHz)
  - ✦ include the unknowns in the covariance matrix (non-diagonal, low rank terms), (eg, beam shape)
- Expected **systematic effects**:
  - ✦ model their impact on C_ℓ, (eg, beam induced T to P leakage in 2017),
  - ✦ if not, find a template to be fit on the data, (eg, beam induced T to P leakage in 2015),
  - ✦ if not, find an upper limit on their impact.
- To assess **robustness** of the results:
  - ✦ compare various approaches, options, codes, hypotheses, …
    - 5 pipelines at high-ℓ, 4 CMB-only maps
  - ✦ compare to simulations,
  - ✦ test consistency across frequency, data splits, …
- **The analysis has to be repeated many, many times: need for a fast and robust pipeline**

Bibliography

Hivon et al, 2017 (QuickPol) 2017A&A...598A..25H

Hu et al, 2003PhRvD..67d3004H

Planck 2015-XI, 2016 2016A&A…594A..11P

Takakura et al, 2017 (Polarbear) 2017JCAP...05..008T

Back to page 1

The scientific results that we present today are a product of the Planck Collaboration, including individuals from more than 100 scientific institutes in Europe, the USA and Canada.

Planck is a project of the European Space Agency, with instruments provided by two scientific Consortia funded by ESA member states (in particular the lead countries: France and Italy) with contributions from NASA (USA), and telescope reflectors provided in a collaboration between ESA and a scientific Consortium led and funded by Denmark.